Usta, M. A. (2024). A Mathematical Review Study on Dynamical Models of Symmetrical Three-Phase Induction Machine in Various Reference Frames. *The Black Sea Journal of Sciences*, 14(3), 1401-1430.

The Black Sea Journal of Sciences, 14(3), 1401-1430, 2024. DOI: 10.31466/kfbd.1472193

KFBD

Karadeniz Fen Bilimleri Dergisi
The Black Sea Journal of Sciences
ISSN (Online): 2564-7377 https://dergipark.org.tr/tr/pub/kfbd

Araştırma Makalesi / Research Article

A Mathematical Review Study on Dynamical Models of Symmetrical Three-Phase Induction Machine in Various Reference Frames

Mehmet Ali USTA[1*]

Abstract

This paper presents dynamic models of a three-phase induction machine in various reference frames widely employed in alternating-current (ac) machine analysis. The main objective is to derive and explain the machine model in relatively basic terms by using the idea of rotating reference frame theory. Many matrix manipulations and complex frame-to-frame transformations performed to obtain an advanced model from primitive dynamical equations are presented in a more compact and easy-to-understand way. Therefore, this paper reviews a detailed, yet simple and understandable mathematical background on the dynamic models of the induction machine. Furthermore, a unified and broadly applicable simulation model is proposed for simulating the dynamic behavior of the machine in any desired reference frame. The simulation model has also a modular and user-friendly structure. For the simulation studies, Matlab/Simulink environment is preferred due to its popularity. A Simulink machine model with several subsystems is explicitly given. The simulation study is realized for a small power induction machine operating under both load and no-load conditions. The variations of three-phase currents, electromagnetic torque, and rotor mechanical speed as well as the rotor flux-linkage components are shown. The key features of each reference frame are discussed, especially through the measured rotor flux-linkage components.

Keywords: Induction machine, Reference frame theory, Dynamic model, Simulation model.

Simetrik Üç Fazlı Asenkron Makinanın Çeşitli Referans Çerçevelerinde Dinamik Modelleri Üzerine Matematiksel Bir İnceleme Çalışması

Öz

Bu makale, alternatif akım (aa) makine analizinde yaygın olarak kullanılan çeşitli referans çerçevelerinde üç fazlı asenkron makinanın dinamik modellerini sunmaktadır. Temel amaç, dönen referans çerçeve teorisi fikrini kullanarak makina modelini nispeten basit terimlerle türetmek ve açıklamaktır. İlkel dinamik denklemlerden gelişmiş bir model elde etmek için gerçekleştirilen birçok matris manipülasyonu ve karmaşık çerçeveden çerçeveye dönüşümler, daha kompakt ve anlaşılması kolay bir şekilde sunulmaktadır. Bu nedenle, bu makale asenkron makinanın dinamik modellerine ilişkin ayrıntılı, ancak basit ve anlaşılır bir matematiksel arka planı gözden geçirmektedir. Bundan başka, makinanın dinamik davranışını istenen herhangi bir referans çerçevesinde simüle etmek için birleşik ve geniş çapta uygulanabilir bir simülasyon modeli önerilmektedir. Simülasyon modeli aynı zamanda modüler ve kullanıcı dostu bir yapıya sahiptir. Simülasyon çalışmalarında popülerliği nedeniyle Matlab/Simulink ortamı tercih edilmektedir. Birkaç alt sisteme sahip bir Simulink makina modeli açıkça verilmiştir. Simülasyon çalışması hem yük hem de yüksüz koşullar altında çalışan küçük güçlü bir asenkron makina için gerçekleştirilmiştir. Üç fazlı akımların, elektromanyetik torkun ve rotor mekanik hızının yanı sıra rotor akı bileşenlerinin değişimleri gösterilmektedir. Her bir referans çerçevesinin temel özellikleri, özellikle ölçülen rotor akı bileşenleri aracılığıyla tartışılmaktadır.

Anahtar Kelimeler: Asenkron makina, Referans çerçeve teorisi, Dinamik model, Benzetim modeli.

[1]Giresun University, Department of Computer Engineering, Giresun, Turkey, mehmet.usta@giresun.edu.tr

[*]Sorumlu Yazar/Corresponding Author
Geliş/Received: 22.04.2024 **Kabul/Accepted:** 08.08.2024 **Yayın/Published:** 15.09.2024

1. Introduction

The induction machine is used extensively in a great number of industrial applications, especially in variable-speed drives. They are considered to be the workhorses of the electric power industry (Vas, 1998; Krause et al., 2002). This is because it has many needful features in comparison with a direct-current (dc) machine, e.g., simple and rugged structure, low-cost, low-maintenance requirement, high efficiency, reliability, and so on. However, unlike a dc machine, the control of an induction machine is quite sophisticated, and they require various complex types of hardware and software equipment to solve its control problem. So far, there have been many advances in power converters, microprocessor technologies, and control techniques to fulfill these control requirements. Therefore, induction motor drives have now gained a considerable place in the world market and replaced variable-speed dc drives.

The dynamic model of the induction machine is used to simulate the transient and steady-state behaviors of the machine not only under balanced conditions but also under various unbalanced conditions. The dynamic model is also necessary to develop and analyze the control structures. The dynamic behavior of any rotary machine is defined by a system of differential equations. In ac machines, these equations contain time-varying coefficients and are inherently nonlinear. The reason is that the mutual inductances change in the form of a function of rotor speed as the rotor phase windings rotate relative to the stator. Reference frame theory is used to eliminate all these time-dependent inductances and hence transform them into a linear system. The main idea of the theory is based on the redefinition of machine variables (rotor and stator side voltages, currents, flux-linkages) with their corresponding equivalents in the desired reference frames. Herein, a “reference frame” is referred to as a set of direct and quadrature axes (dq axes) that rotate at a particular angular speed (or do not rotate when angular speed is zero). The development of the reference frame theory can be given as follows:

- The stator variables were transferred into a reference frame rotating with the rotor (Park, 1929). In other words, all three-phase abc (rotor and stator) quantities were referred to a dq^r reference frame fixed to the rotor. The Park’s transformation was first applied to a synchronous machine. Then, Brereton et al. (1957) was used it in a similar way to analyze a symmetrical induction machine. This reference frame is commonly called the rotor reference frame.
- The rotor variables were transferred into a reference frame which is stationary with respect to the stator (Stanley, 1938). In this case, all three-phase abc (rotor and stator) quantities were referred to a dq^0 reference frame fixed to the stator. This reference frame is commonly called the stationary reference frame.

- The stator and rotor variables were transferred into a reference frame rotating in synchronism with the rotating magnetic field (Kron, 1951). In other words, all three-phase abc (rotor and stator) quantities were referred to a dq^s reference frame rotating with synchronous speed. This reference frame is commonly called the synchronous reference frame.

Initially, it was believed that the three reference frames given above was different, and these were applied individually to help with the study of ac machines for a long time. However, Krause and Thomas (1965) described that all these reference frames are contained in one general reference frame. This is called the "arbitrary reference frame" in which the dq axes rotate at an arbitrary speed. Other reference frames correspond to specific applications of this arbitrary reference frame. That is, the dq axes are rotated at a specified speed rather than an arbitrary speed. As mentioned above, there are three reference frame speeds in the analysis of ac machine. These are; (i) (stationary reference frame) the dq axes do not rotate, (ii) (synchronous reference frame) the dq axes rotate at synchronous speed, and (iii) (rotor reference frame) the dq axes rotate at rotor speed. The readers can refer to (Lee et al., 1984; Q'Rourke et al., 2019) for a more comprehensive description of reference frames. As a result, a unified model that can be easily arranged to simulate an induction machine in any desired reference frame is developed in (Krause and Thomas, 1965). In the following years, an analytical method for introducing stator and rotor leakage inductance saturation into this simulation model is developed (Lipo and Consoli, 1984). In addition, several linear and nonlinear models suitable for transient and steady-state analysis are also presented (Slemon, 1988).

The machine model based on the theory of rotating reference frame is quite proper for the study of transient and steady-state behaviors and the design of control structures. It has proven to be reliable and accurate by many studies. To this end, many graduate-level textbooks (Novotny and Lipo, 1996; Vas, 1998; Krishnan, 2001; Krause et al., 2002; Bose, 2002; Wack, 2011; Abu-Rub et al., 2012; Melkebeek, 2018) discuss and present the reference frame theory and the dq axes machine model in different ways. Some textbooks even show in detail how to perform complex mathematical operations to derive an advanced model from primitive dynamical equations. This paper aims to derive the dynamic models of the induction machine in a more compact and simple way. In addition, this study complements previous studies due to the following contributions:

- This study first obtains all the primitive dynamic equations step by step before the machine model is expressed in the arbitrary reference frame. These are provided from an interrelated three-step workflow. Each stage corresponds respectively to "three-phase model", "two-phase slip-ring model" and "two-phase commutator model" of the machine. Subsequently, the general machine model in the arbitrary reference frame is obtained, and the ready-to-use advanced model is presented. Throughout this process, all the mathematical operations are given in a simple and compact form. Hence, it can be said that a simple and understandable mathematical background on the dynamic models of the induction machine is reviewed by this study.

- This study specifically focuses on the arbitrary reference frame, and how this relates to other reference frames. It is introduced how to transfer the machine model from the arbitrary reference frame to other reference frames. The key features of each reference frame are briefly highlighted.
- This study presents three distinct state-space models for the induction machine. Each state-space model is given in a compact form on the arbitrary reference frame. From this point of view, it is shown that an induction machine can be defined by a total of nine dynamic models.
- This study presents a general simulation block diagram that is valid for all the reference frames. Various software packages can be used for simulation studies such as Pscipe (Akherraz, 1997), Labview (Li and Hu, 2010), and Matlab (Shi et al., 1997; Ozpineci and Tolbert, 2003; Abu-Rub et al., 2012). Among them, Matlab/Simulink environment is very popular, and it was preferred for simulation studies. The simulation model is divided into many sub-models. It allows us to access all the machine variables for monitoring, comparison, and control purposes. Therefore, it has a modular and user-friendly structure. The simulation model can be easily altered so that it can be simulated in three different reference frames without any modifications to sub-models. This shows that the simulation model has a unified and universally applicable structure.

This paper is organized into eight sections. In Section 2, the primitive machine models are presented, and the advanced machine model is obtained in the arbitrary reference frame. Sections 3 and 4 present the space-phasor forms of voltage and flux-linkage equations, and three different state-space models, respectively. Section 5 discusses the mechanism of electromagnetic torque production in ac machines, and the torque equations are given in different forms. Section 6 explains widely used reference frames in the analysis of ac machines. Sections 7 and 8 present simulation studies, obtained results, and discussions. Finally, the drawn conclusions are evaluated in Section 9.

2. Modeling of Induction Machine

Fig. 1 illustrates the schematic view of an induction machine under consideration. In order to simplify the analysis and modeling stages, the following assumptions are considered:

- It has a symmetrical two-pole structure with a smooth air-gap.
- Stator and rotor have three-phase windings placed by 120 electrical degrees from each other.

- The phase windings are composed of distributed windings that generate sinusoidal magneto-motive force (mmf) waves centered on the magnetic axes of the corresponding phases. The effects of mmf space harmonics are neglected.
- The iron losses and end-effects are neglected, such that the flux density is radial in the air-gap and the iron parts have infinite permeability.

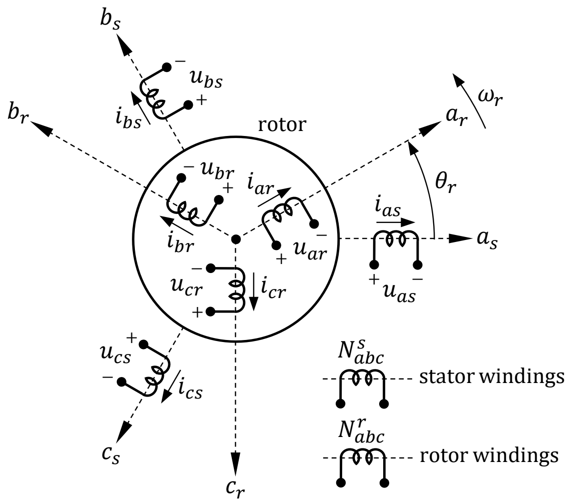

Figure 1. Schematic view of an elementary symmetrical three-phase machine

2.1. Three-Phase Model

The first step in modeling is to obtain the three-phase stator and rotor voltage equations in three-phase (natural) reference frames. Therefore, the stator voltage equations are defined in the stationary reference frame fixed to the stator, and the rotor voltage equations are defined in the rotating reference frame fixed to the rotor. The three-phase stator and rotor voltage equations are as follows:

$$\begin{aligned}\bar{u}_{abcs} &= \mathbf{R}_s \bar{\iota}_{abcs} + \rho \bar{\psi}_{abcs} \\ \bar{u}_{abcr} &= \mathbf{R}_r \bar{\iota}_{abcr} + \rho \bar{\psi}_{abcr}\end{aligned} \tag{1}$$

where $\rho = d/dt$ is the differential operator. The stator and rotor resistance matrices are

$$\mathbf{R}_s = \begin{bmatrix} R_s & 0 & 0 \\ 0 & R_s & 0 \\ 0 & 0 & R_s \end{bmatrix} \;,\; \mathbf{R}_r = \begin{bmatrix} R_r & 0 & 0 \\ 0 & R_r & 0 \\ 0 & 0 & R_r \end{bmatrix} \tag{2}$$

where R_s and R_r are the resistances of a stator and rotor phase winding, respectively. $\bar{u}_{abcx}$, $\bar{\iota}_{abcx}$, and $\bar{\psi}_{abcx}$ (the subscript x is s or r) denote the column matrices for the stator and rotor quantities.

These are defined by $\bar{u}_{abcs} = [u_{as}\ u_{bs}\ u_{cs}]^t$, $\bar{u}_{abcr} = [u_{ar}\ u_{br}\ u_{cr}]^t$, $\bar{\imath}_{abcs} = [i_{as}\ i_{bs}\ i_{cs}]^t$, $\bar{\imath}_{abcr} = [i_{ar}\ i_{br}\ i_{cr}]^t$, $\bar{\psi}_{abcs} = [\psi_{as}\ \psi_{bs}\ \psi_{cs}]^t$, and $\bar{\psi}_{abcr} = [\psi_{ar}\ \psi_{br}\ \psi_{cr}]^t$. Also, the stator and rotor flux-linkages are defined by

$$\begin{aligned} \bar{\psi}_{abcs} &= \mathbf{L}_{abcs(s)}\bar{\imath}_{abcs} + \mathbf{L}_{abcs(r)}\bar{\imath}_{abcr} \\ \bar{\psi}_{abcr} &= \mathbf{L}_{abcr(s)}\bar{\imath}_{abcs} + \mathbf{L}_{abcr(r)}\bar{\imath}_{abcr} \end{aligned} \tag{3}$$

There is no change in the magnetic circuit for a machine with a smooth air-gap when its rotor rotates. Thus, the self-inductance of a stator phase winding $\bar{L}_s$ and the mutual inductance between two stator windings $\bar{M}_s$ do not depend on the rotor electrical angle θ_r. Then, the inductance matrix between the stator windings $\mathbf{L}_{abcs(s)}$ is

$$\mathbf{L}_{abcs(s)} = \begin{bmatrix} \bar{L}_s & \bar{M}_s & \bar{M}_s \\ \bar{M}_s & \bar{L}_s & \bar{M}_s \\ \bar{M}_s & \bar{M}_s & \bar{L}_s \end{bmatrix} \tag{4}$$

and

$$\bar{L}_s = L_{ls} + L_{ms} \quad , \quad \bar{M}_s = L_{ms}\cos\left(\frac{2\pi}{3}\right) = -\frac{1}{2}L_{ms} \tag{5}$$

where L_{ls} and L_{ms} are the leakage inductance and magnetizing inductance of a stator phase winding, respectively. Similarly, the self-inductance of a rotor phase winding $\bar{L}_r$ and the mutual inductance between two rotor windings $\bar{M}_r$ are independent of the rotor electrical angle θ_r. Then, the inductance matrix between the rotor windings $\mathbf{L}_{abcr(r)}$ is

$$\mathbf{L}_{abcr(r)} = \begin{bmatrix} \bar{L}_r & \bar{M}_r & \bar{M}_r \\ \bar{M}_r & \bar{L}_r & \bar{M}_r \\ \bar{M}_r & \bar{M}_r & \bar{L}_r \end{bmatrix} \tag{6}$$

and

$$\bar{L}_r = L_{lr} + L_{mr} \quad , \quad \bar{M}_r = L_{mr}\cos\left(\frac{2\pi}{3}\right) = -\frac{1}{2}L_{mr} \tag{7}$$

where L_{lr} and L_{mr} are the leakage inductance and magnetizing inductance of a rotor phase winding, respectively. On the contrary, since the rotor phase windings rotate relative to the stator, the mutual inductance between the rotor and stator phase windings change depending on the rotor electrical angle θ_r. Then, the rotor-stator mutual inductance matrix $\mathbf{L}_{abcs(r)}$ is

$$\mathbf{L}_{abcs(r)} = \begin{bmatrix} \bar{M}_{sr}\cos\theta_1 & \bar{M}_{sr}\cos\theta_2 & \bar{M}_{sr}\cos\theta_3 \\ \bar{M}_{sr}\cos\theta_3 & \bar{M}_{sr}\cos\theta_1 & \bar{M}_{sr}\cos\theta_2 \\ \bar{M}_{sr}\cos\theta_2 & \bar{M}_{sr}\cos\theta_3 & \bar{M}_{sr}\cos\theta_1 \end{bmatrix} \tag{8}$$

where $\bar{M}_{sr}$ is the maximum value of the stator-rotor mutual inductance. The angles θ_1, θ_2 and θ_3 are defined as $\theta_1 = \theta_r$, $\theta_2 = \theta_r + 2\pi/3$ and $\theta_3 = \theta_r - 2\pi/3$. For the number of pole-pairs $p = 1$, θ_r is equal to θ_m, where θ_m is the rotor mechanical angle. A similar definition can be made for the stator-rotor mutual inductance matrix $\mathbf{L}_{abcr(s)}$. Due to the symmetry of the machine structure, it is given by

$$\mathbf{L}_{abcr(s)} = \mathbf{L}^t_{abcs(r)} \tag{9}$$

On the other hand, the relationship between the magnetizing inductance of the stator or rotor winding (L_{ms} or L_{mr}) and the maximum value of the mutual inductance $\bar{M}_{sr}$ is formulated by

$$L_{ms} = N\bar{M}_{sr} \quad , \quad L_{mr} = N\bar{M}_{sr} \tag{10}$$

where N is the effective turn ratio and is equal to N^s_{abc}/N^r_{abc}. It also follows that $L_{ms} = N^2 L_{mr}$. For convenience, the stator and rotor voltage equations of a three-phase machine can be combined into a single matrix form as follows:

$$\bar{u}_{abc} = \mathbf{R}\bar{\imath}_{abc} + \frac{d}{dt}\bar{\psi}_{abc} \tag{11.a}$$

where $\bar{u}_{abc} = [\bar{u}_{abcs}\ \bar{u}_{abcr}]^t$, $\bar{\imath}_{abc} = [\bar{\imath}_{abcs}\ \bar{\imath}_{abcr}]^t$, $\bar{\psi}_{abc} = [\bar{\psi}_{abcs}\ \bar{\psi}_{abcr}]^t$. Since $\bar{\psi}_{abc} = \mathbf{L}_{abc}\bar{\imath}_{abc}$, Eq. (11.a) can be rearranged by

$$\bar{u}_{abc} = (\mathbf{R} + \rho\mathbf{L}_{abc})\bar{\imath}_{abc} \tag{11.b}$$

and

$$\mathbf{R} = \begin{bmatrix} \mathbf{R}_s & \mathbf{0} \\ \mathbf{0} & \mathbf{R}_r \end{bmatrix} \quad , \quad \mathbf{L}_{abc} = \begin{bmatrix} \mathbf{L}_{abcs(s)} & \mathbf{L}_{abcs(r)} \\ \mathbf{L}_{abcs(r)}^t & \mathbf{L}_{abcr(r)} \end{bmatrix}$$

The mathematical model of induction machine in three-phase reference frame is represented by Eq. (11.b). In this model, the impedance matrix $\mathbf{Z}_{abc} = \mathbf{R} + \rho\mathbf{L}_{abc}$ is nonlinear, and contains variable, time-dependent coefficients, because the rotor angle varies with time. Consequently, it is not possible to solve the system of differential equations derived from this fully coupled impedance matrix.

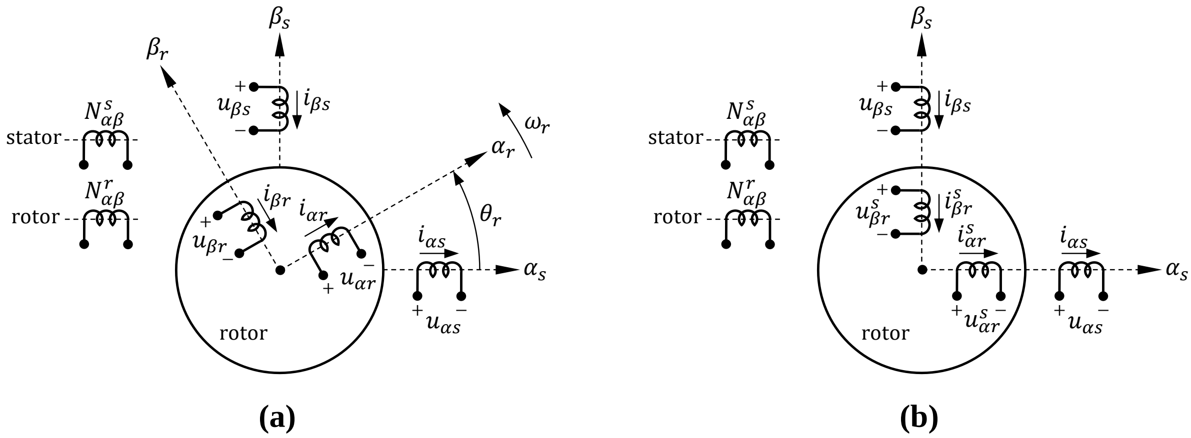

Figure 2. Schematic view of two-phase machine models; **(a)** two-phase slip-ring model, **(b)** two-phase commutator model

2.2. Two-Phase Slip-Ring Model

The two-phase slip-ring model is obtained as shown in Fig. 2a when the three-phase quantities (voltages, currents, flux-linkages) in the previous voltage equations are replaced by their two-phase equivalents expressed in the same reference frame. In this case, assuming that there are no zero-sequence voltages and currents on the stator and rotor, only four voltage equations can be written in total. They correspond to alpha- and beta-axis ($\alpha\beta$ axes) stator and rotor voltage equations. The phase transformation matrix $\mathbf{C}_1$ is applied to the three-phase quantities to obtain the two-phase equivalent quantities. The transformation matrix $\mathbf{C}_1$ is

$$\mathbf{C}_1 = c \cdot \mathbf{M} \tag{12}$$

where

$$\mathbf{M}=\begin{bmatrix} 1 & -\frac{1}{2} & -\frac{1}{2} \\ 0 & \frac{\sqrt{3}}{2} & -\frac{\sqrt{3}}{2} \\ \frac{1}{\sqrt{2}} & \frac{1}{\sqrt{2}} & \frac{1}{\sqrt{2}} \end{bmatrix}$$

and c is a constant. For the power-invariant case, c is equal to $\sqrt{2/3}$. However, for the non-power-invariant case, $c=2/3$. Then, the relationship between the two-phase voltage components and their three-phase components is defined by

$$\begin{bmatrix} \bar{u}_{\alpha\beta s} \\ \bar{u}_{\alpha\beta r} \end{bmatrix} = \begin{bmatrix} \mathbf{C}_1 & \mathbf{0} \\ \mathbf{0} & \mathbf{C}_1 \end{bmatrix} \begin{bmatrix} \bar{u}_{abcs} \\ \bar{u}_{abcr} \end{bmatrix} \tag{13}$$

where $\bar{u}_{\alpha\beta s}=\left[u_{\alpha s}\ u_{\beta s}\right]^t$ and $\bar{u}_{\alpha\beta r}=\left[u_{\alpha r}\ u_{\beta r}\right]^t$. It should be noted that the zero-sequence voltages on the stator and rotor are ignored. This means that the third row of $\mathbf{M}$ is discarded for the above transformation. Similar transformations hold for the stator and rotor currents.

$$\begin{bmatrix} \bar{\imath}_{\alpha\beta s} \\ \bar{\imath}_{\alpha\beta r} \end{bmatrix} = \begin{bmatrix} \mathbf{C}_1 & \mathbf{0} \\ \mathbf{0} & \mathbf{C}_1 \end{bmatrix} \begin{bmatrix} \bar{\imath}_{abcs} \\ \bar{\imath}_{abcr} \end{bmatrix} \tag{14}$$

where $\bar{\imath}_{\alpha\beta s}=\left[i_{\alpha s}\ i_{\beta s}\right]^t$ and $\bar{\imath}_{\alpha\beta r}=\left[i_{\alpha r}\ i_{\beta r}\right]^t$.

The inverse transformations are performed by

$$\bar{u}_{abc}=\mathbf{C}_{11}^{-1}\bar{u}_{\alpha\beta} \quad , \quad \bar{\imath}_{abc}=\mathbf{C}_{11}^{-1}\bar{\imath}_{\alpha\beta} \tag{15}$$

where $\bar{u}_{\alpha\beta}=\left[\bar{u}_{\alpha\beta s}\ \bar{u}_{\alpha\beta r}\right]^t$ and $\bar{\imath}_{\alpha\beta}=\left[\bar{\imath}_{\alpha\beta s}\ \bar{\imath}_{\alpha\beta r}\right]^t$. Also, $\mathbf{C}_{11}$ is

$$\mathbf{C}_{11}=\begin{bmatrix} \mathbf{C}_1 & \mathbf{0} \\ \mathbf{0} & \mathbf{C}_1 \end{bmatrix} = c\cdot\begin{bmatrix} \mathbf{M} & \mathbf{0} \\ \mathbf{0} & \mathbf{M} \end{bmatrix}$$

and for the power-invariant case, the inverse of $\mathbf{C}_{11}$ is given by,

$$\mathbf{C}_{11}^{-1}=\mathbf{C}_{11}^{t}=\sqrt{\frac{2}{3}}\begin{bmatrix} \mathbf{M}^t & \mathbf{0} \\ \mathbf{0} & \mathbf{M}^t \end{bmatrix}$$

and for the non-power-invariant case, it is obtained by

$$\mathbf{C}_{11}^{-1} = \begin{bmatrix} \mathbf{M}^t & \mathbf{0} \\ \mathbf{0} & \mathbf{M}^t \end{bmatrix}$$

Thus, by substituting Eq. (15) into Eq. (11.b) and after some algebraic manipulation, the machine model takes the following form:

$$\bar{u}_{\alpha\beta} = \mathbf{R}\bar{\imath}_{\alpha\beta} + \frac{d}{dt}\left(\mathbf{L}_{\alpha\beta}\bar{\imath}_{\alpha\beta}\right) \tag{16}$$

where the total inductance matrix is

$$\mathbf{L}_{\alpha\beta} = \mathbf{C}_{11}\mathbf{L}_{abc}\mathbf{C}_{11}^{-1} = \begin{bmatrix} L_s & 0 & M_{sr}\cos\theta_r & -M_{sr}\sin\theta_r \\ 0 & L_s & M_{sr}\sin\theta_r & M_{sr}\cos\theta_r \\ M_{sr}\cos\theta_r & M_{sr}\sin\theta_r & L_r & 0 \\ -M_{sr}\sin\theta_r & M_{sr}\cos\theta_r & 0 & L_r \end{bmatrix} \tag{17}$$

and L_s, L_r, and M_{sr} are obtained by using Eqs. (5) and (7) as

$$\begin{aligned} &L_s = \bar{L}_s - \bar{M}_s = L_{ls} + \frac{3}{2}L_{ms} \quad , \quad L_r = \bar{L}_r - \bar{M}_r = L_{lr} + \frac{3}{2}L_{mr} \\ &M_{sr} = \frac{3}{2}\bar{M}_{sr} \end{aligned} \tag{18}$$

where L_s and L_r represent the total three-phase stator and rotor inductances, respectively. M_{sr} is the three-phase magnetizing inductance.

The two-phase slip-ring model of the induction machine is represented by Eq. (16). In this model, the total inductance matrix still contains the rotor angle. It is noted that when the phase transformation is applied to the three-phase model, the stationary three-phase is reduced to the two-phase fixed to the stator while the rotating three-phase is reduced to the two-phase fixed to the rotor. Therefore, the transformed impedance matrix $\mathbf{Z}_{\alpha\beta} = \mathbf{R} + \rho\mathbf{L}_{\alpha\beta}$ includes time-dependent terms even if all of the machine parameters are considered to be constant.

2.3. Two-Phase Commutator Model

The two-phase commutator model is obtained as shown in Fig. 2b if the rotor quantities of the two-phase slip-ring model are transferred into a new reference frame fixed to the stator, providing that the stator quantities are unchanged. In this case, in the absence of the zero-sequence components, there will still be four voltage equations, but these resulting equations are now purified from the rotor angle. The rotor voltages and currents are transferred to the pseudo-stationary windings fixed to the stator by the transformation matrix $\mathbf{C}_2$. The transformation matrix $\mathbf{C}_2$ is

$$\mathbf{C}_2 = \begin{bmatrix} \cos\theta_r & -\sin\theta_r \\ \sin\theta_r & \cos\theta_r \end{bmatrix} \tag{19}$$

Then, the corresponding stator and rotor quantities to the commutator model are obtained by

$$\begin{bmatrix} \bar{u}_{\alpha\beta s} \\ \bar{u}^s_{\alpha\beta r} \end{bmatrix} = \begin{bmatrix} \mathbf{I} & \mathbf{0} \\ \mathbf{0} & \mathbf{C}_2 \end{bmatrix} \begin{bmatrix} \bar{u}_{\alpha\beta s} \\ \bar{u}_{\alpha\beta r} \end{bmatrix} \quad , \quad \begin{bmatrix} \bar{\imath}_{\alpha\beta s} \\ \bar{\imath}^s_{\alpha\beta r} \end{bmatrix} = \begin{bmatrix} \mathbf{I} & \mathbf{0} \\ \mathbf{0} & \mathbf{C}_2 \end{bmatrix} \begin{bmatrix} \bar{\imath}_{\alpha\beta s} \\ \bar{\imath}_{\alpha\beta r} \end{bmatrix} \tag{20}$$

where $\bar{u}^s_{\alpha\beta r} = \left[u^s_{\alpha r}\ u^s_{\beta r}\right]^t$ and $\bar{\imath}^s_{\alpha\beta r} = \left[i^s_{\alpha r}\ i^s_{\beta r}\right]^t$. It should be noted that all the stator quantities are already stationary with respect to the stator and no transformations are made for them.

The inverse transformations are performed by

$$\bar{u}_{\alpha\beta} = \mathbf{C}_{22}^{-1} \bar{u}^s_{\alpha\beta} \quad , \quad \bar{\imath}_{\alpha\beta} = \mathbf{C}_{22}^{-1} \bar{\imath}^s_{\alpha\beta} \tag{21}$$

where $\bar{u}^s_{\alpha\beta} = \left[\bar{u}_{\alpha\beta s}\ \bar{u}^s_{\alpha\beta r}\right]^t$ and $\bar{\imath}^s_{\alpha\beta} = \left[\bar{\imath}_{\alpha\beta s}\ \bar{\imath}^s_{\alpha\beta r}\right]^t$. Also, $\mathbf{C}_{22}$ is

$$\mathbf{C}_{22} = \begin{bmatrix} \mathbf{I} & \mathbf{0} \\ \mathbf{0} & \mathbf{C}_2 \end{bmatrix}$$

and $\mathbf{C}_2$ is an orthogonal matrix, that is $\mathbf{C}_{22}^{-1} = \mathbf{C}_{22}^t$. Thus, by substituting Eq. (21) into Eq. (16) and after some algebraic manipulation, the two-phase commutator model is obtained by

$$\bar{u}^s_{\alpha\beta} = \mathbf{R}\bar{\imath}^s_{\alpha\beta} + \mathbf{L}^s_{\alpha\beta} \frac{d}{dt} \bar{\imath}^s_{\alpha\beta} + \mathbf{G}^s_{\alpha\beta} \frac{d\theta_r}{dt} \bar{\imath}^s_{\alpha\beta} \tag{22}$$

where

$$\mathbf{L}^s_{\alpha\beta} = \mathbf{C}_{22} \mathbf{L}_{\alpha\beta} \mathbf{C}_{22}^t = \begin{bmatrix} L_s & 0 & M_{sr} & 0 \\ 0 & L_s & 0 & M_{sr} \\ M_{sr} & 0 & L_r & 0 \\ 0 & M_{sr} & 0 & L_r \end{bmatrix} \tag{23}$$

and

$$\mathbf{G}^{s}_{\alpha\beta}\frac{d\theta_r}{dt} = \mathbf{C}_{22}\frac{d}{dt}\left(\mathbf{L}_{\alpha\beta}\mathbf{C}^{t}_{22}\right)$$

where $d\theta_r/dt = \omega_r$ is the rotor electrical angular speed, and the speed matrix $\mathbf{G}^{s}_{\alpha\beta}$ is

$$\mathbf{G}^{s}_{\alpha\beta} = \begin{bmatrix} 0 & 0 & 0 & 0 \\ 0 & 0 & 0 & 0 \\ 0 & M_{sr} & 0 & L_r \\ -M_{sr} & 0 & -L_r & 0 \end{bmatrix} \tag{24}$$

Eventually, from Eqs. (23) and (24), the two-phase commutator model can be given in a more compact form as follows:

$$\bar{u}^{s}_{\alpha\beta} = \left(\mathbf{R} + \mathbf{L}^{s}_{\alpha\beta}\rho + \mathbf{G}^{s}_{\alpha\beta}\omega_r\right)\bar{\imath}^{s}_{\alpha\beta} \tag{25.a}$$

or it is more explicitly as

$$\begin{bmatrix} u_{\alpha s} \\ u_{\beta s} \\ u^{s}_{\alpha r} \\ u^{s}_{\beta r} \end{bmatrix} = \begin{bmatrix} R_s + L_s\rho & 0 & M_{sr}\rho & 0 \\ 0 & R_s + L_s\rho & 0 & M_{sr}\rho \\ M_{sr}\rho & M_{sr}\omega_r & R_r + L_r\rho & L_r\omega_r \\ -M_{sr}\omega_r & M_{sr}\rho & -L_r\omega_r & R_r + L_r\rho \end{bmatrix} \begin{bmatrix} i_{\alpha s} \\ i_{\beta s} \\ i^{s}_{\alpha r} \\ i^{s}_{\beta r} \end{bmatrix} \tag{25.b}$$

It is seen that the impedance matrix $\mathbf{Z}^{s}_{\alpha\beta} = \mathbf{R} + \mathbf{L}^{s}_{\alpha\beta}\rho + \mathbf{G}^{s}_{\alpha\beta}\omega_r$ in the commutator model does not now include a function dependent on the rotor angle, but only includes the rotor electrical angular speed in the rotor voltage equations. Therefore, this system of differential equations will be linear if all the parameters of the machine are constant.

2.4. Machine Model in Arbitrary Reference Frame

In the two-phase commutator model, the stator and rotor voltage equations are defined relative to a reference frame fixed to the stator (which is often called the stationary reference frame). However, a more general machine model can be obtained when a general (arbitrary) reference frame rotating at an arbitrary angular speed ω_a is used rather than the stationary reference frame. The machine model in the arbitrary reference frame is shown in Fig. 3, where θ_a is the angle between the real axes of the stationary and arbitrary reference frames.

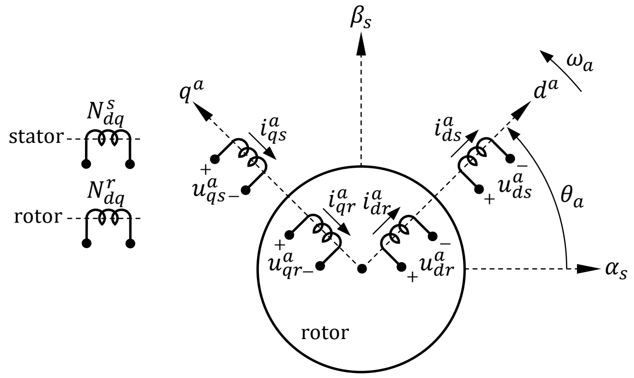

Figure 3. Schematic view of machine model in the arbitrary reference frame

The transformation matrix $\mathbf{C}_3$ is used to transform the stator and rotor quantities in the stationary reference frame into the arbitrary reference frame.

$$\mathbf{C}_3 = \begin{bmatrix} \cos\theta_a & \sin\theta_a \\ -\sin\theta_a & \cos\theta_a \end{bmatrix} \tag{26}$$

and hence, the following can be written:

$$\begin{bmatrix} \bar{u}_{dqs}^a \\ \bar{u}_{dqr}^a \end{bmatrix} = \begin{bmatrix} \mathbf{C}_3 & \mathbf{0} \\ \mathbf{0} & \mathbf{C}_3 \end{bmatrix} \begin{bmatrix} \bar{u}_{\alpha\beta s} \\ \bar{u}_{\alpha\beta r}^s \end{bmatrix} \quad , \quad \begin{bmatrix} \bar{\imath}_{dqs}^a \\ \bar{\imath}_{dqr}^a \end{bmatrix} = \begin{bmatrix} \mathbf{C}_3 & \mathbf{0} \\ \mathbf{0} & \mathbf{C}_3 \end{bmatrix} \begin{bmatrix} \bar{\imath}_{\alpha\beta s} \\ \bar{\imath}_{\alpha\beta r}^s \end{bmatrix} \tag{27}$$

where $\bar{u}_{dqs}^a = \left[u_{ds}^a \ u_{qs}^a\right]^t$, $\bar{u}_{dqr}^a = \left[u_{dr}^a \ u_{qr}^a\right]^t$, $\bar{\imath}_{dqs}^a = \left[i_{ds}^a \ i_{qs}^a\right]^t$, and $\bar{\imath}_{dqr}^a = \left[i_{dr}^a \ i_{qr}^a\right]^t$.

The inverse transformations are performed by

$$\bar{u}_{\alpha\beta}^s = \mathbf{C}_{33}^{-1}\bar{u}_{dq}^a \quad , \quad \bar{\imath}_{\alpha\beta}^s = \mathbf{C}_{33}^{-1}\bar{\imath}_{dq}^a \tag{28}$$

where $\bar{u}_{dq}^a = \left[\bar{u}_{dqs}^a \ \bar{u}_{dqr}^a\right]^t$ and $\bar{\imath}_{dq}^a = \left[\bar{\imath}_{dqs}^a \ \bar{\imath}_{dqr}^a\right]^t$. Also, $\mathbf{C}_{33}$ is

$$\mathbf{C}_{33} = \begin{bmatrix} \mathbf{C}_3 & \mathbf{0} \\ \mathbf{0} & \mathbf{C}_3 \end{bmatrix}$$

and $\mathbf{C}_{33}$ is an orthogonal matrix, that is $\mathbf{C}_{33}^{-1} = \mathbf{C}_{33}^t$. Thus, by substituting Eq. (28) into Eq. (22) and after some algebraic manipulation, the machine model in the arbitrary reference frame is obtained by

$$\bar{u}_{dq}^a = \mathbf{R}\bar{\imath}_{dq}^a + \mathbf{L}_{dq}^a \frac{d}{dt}\bar{\imath}_{dq}^a + \left(\mathbf{G}_{dq(\omega_a)}^a \frac{d\theta_a}{dt} + \mathbf{G}_{dq(\omega_r)}^a \frac{d\theta_r}{dt}\right)\bar{\imath}_{dq}^a \tag{29}$$

where $\mathbf{L}_{dq}^{a} = \mathbf{L}_{\alpha\beta}^{s}$, $\mathbf{G}_{dq(\omega_r)}^{a} = \mathbf{G}_{\alpha\beta}^{s}$ and

$$\mathbf{G}_{dq(\omega_a)}^{a} \frac{d\theta_a}{dt} = \mathbf{C}_{33} \mathbf{L}_{\alpha\beta}^{s} \frac{d}{dt} \mathbf{C}_{33}^{t}$$

where $d\theta_a/dt = \omega_a$ is the arbitrary angular speed and the speed matrix $\mathbf{G}_{dq(\omega_a)}^{a}$ is

$$\mathbf{G}_{dq(\omega_a)}^{a} = \begin{bmatrix} 0 & -L_s & 0 & -M_{sr} \\ L_s & 0 & M_{sr} & 0 \\ 0 & -M_{sr} & 0 & -L_r \\ M_{sr} & 0 & L_r & 0 \end{bmatrix} \tag{30}$$

Consequently, the machine model can be written more explicitly from Eq. (29) as follows:

$$\begin{bmatrix} u_{ds}^{a} \\ u_{qs}^{a} \\ u_{dr}^{a} \\ u_{qr}^{a} \end{bmatrix} = \begin{bmatrix} R_s + L_s\rho & -L_s\omega_a & M_{sr}\rho & -M_{sr}\omega_a \\ L_s\omega_a & R_s + L_s\rho & M_{sr}\omega_a & M_{sr}\rho \\ M_{sr}\rho & -M_{sr}(\omega_a - \omega_r) & R_r + L_r\rho & -L_r(\omega_a - \omega_r) \\ M_{sr}(\omega_a - \omega_r) & M_{sr}\rho & L_r(\omega_a - \omega_r) & R_r + L_r\rho \end{bmatrix} \begin{bmatrix} i_{ds}^{a} \\ i_{qs}^{a} \\ i_{dr}^{a} \\ i_{qr}^{a} \end{bmatrix} \tag{31}$$

In the above model, u_{dr}^{a}, u_{qr}^{a} and i_{dr}^{a}, i_{qr}^{a} are the voltage and current quantities on the rotor side. To produce the final per-phase equivalent circuit for an induction machine, it is necessary to refer the quantities of the rotor side to the stator side. As in an ordinary transformer, the voltages and currents on the rotor side can be referred to the stator side by means of the effective turn ratio of the machine.

$$\bar{u}_{dqr}^{a} = \frac{N_{dq}^{r}}{N_{dq}^{s}} \bar{u}_{dqr}^{a\prime} \quad , \quad \bar{\imath}_{dqr}^{a} = \frac{N_{dq}^{s}}{N_{dq}^{r}} \bar{\imath}_{dqr}^{a\prime} \tag{32}$$

where

$$\frac{N_{abc}^{s}}{N_{abc}^{r}} = \frac{N_{\alpha\beta}^{s}}{N_{\alpha\beta}^{r}} = \frac{N_{dq}^{s}}{N_{dq}^{r}} = N$$

It should be noted that the effective turn ratio N is never unchanged, no matter which axis transformation is applied to the machine model. As mentioned earlier, Eq. (31) holds for a machine with a symmetrical two-pole structure, i.e., $p = 1$ and $\omega_r = \omega_m$, where ω_m is the rotor mechanical angular speed. When $p > 1$, the rotor electrical angular speed ω_r is replaced by $p\omega_m$. Then, for $p > 1$ and the manipulation of Eq. (31) with Eq. (32) gives

$$\begin{bmatrix} u_{ds}^{a} \\ u_{qs}^{a} \\ u_{dr}^{a'} \\ u_{qr}^{a'} \end{bmatrix} = \begin{bmatrix} R_s + L_s\rho & -L_s\omega_a & L_m\rho & -L_m\omega_a \\ L_s\omega_a & R_s + L_s\rho & L_m\omega_a & L_m\rho \\ L_m\rho & -L_m(\omega_a - p\omega_m) & R_r' + L_r'\rho & -L_r'(\omega_a - p\omega_m) \\ L_m(\omega_a - p\omega_m) & L_m\rho & L_r'(\omega_a - p\omega_m) & R_r' + L_r'\rho \end{bmatrix} \begin{bmatrix} i_{ds}^{a} \\ i_{qs}^{a} \\ i_{dr}^{a'} \\ i_{qr}^{a'} \end{bmatrix} \tag{33}$$

where $L_m = NM_{sr}$, and by using Eq. (10) and Eq. (18), it can be written by

$$L_m = \frac{3}{2}L_{ms} \quad \vee \quad L_m = N^2\frac{3}{2}L_{mr}$$

and also, we can write

$$R_r' = N^2R_r \quad , \quad L_r' = N^2L_r = N^2\left(L_{lr} + \frac{3}{2}L_{mr}\right) = L_{lr}' + L_m$$

$$L_s = L_{ls} + \frac{3}{2}L_{ms} = L_{ls} + L_m$$

where the $'$ superscript represents the rotor quantities reduced to the stator side. On the other hand, since $\bar{\psi}_{dq}^{a} = \mathbf{L}_{dq}^{a}\bar{\imath}_{dq}^{a}$ in Eq. (29), the stator and rotor flux-linkages are given by

$$\begin{bmatrix} \bar{\psi}_{dqs}^{a} \\ \bar{\psi}_{dqr}^{a} \end{bmatrix} = \mathbf{L}_{dq}^{a} \begin{bmatrix} \bar{\imath}_{dqs}^{a} \\ \bar{\imath}_{dqr}^{a} \end{bmatrix} \tag{34}$$

where $\bar{\psi}_{dqs}^{a} = \left[\psi_{ds}^{a} \;\; \psi_{qs}^{a}\right]^t$ and $\bar{\psi}_{dqr}^{a} = \left[\psi_{dr}^{a} \;\; \psi_{qr}^{a}\right]^t$. ψ_{dr}^{a}, ψ_{qr}^{a} and i_{dr}^{a}, i_{qr}^{a} are the flux-linkage and current quantities on the rotor side. When these rotor quantities are referred to the stator side by using

$$\bar{\psi}_{dqr}^{a} = \frac{1}{N}\bar{\psi}_{dqr}^{a'} \quad , \quad \bar{\imath}_{dqr}^{a} = N\bar{\imath}_{dqr}^{a'}$$

the flux-linkages reduced to the stator side are

$$\begin{bmatrix} \bar{\psi}_{dqs}^{a} \\ \bar{\psi}_{dqr}^{a'} \end{bmatrix} = \mathbf{L}_{dq}^{a'} \begin{bmatrix} \bar{\imath}_{dqs}^{a} \\ \bar{\imath}_{dqr}^{a'} \end{bmatrix} \tag{35}$$

where since $\mathbf{L}_{dq}^{a}=\mathbf{L}_{\alpha\beta}^{s}$, we obtain

$$\mathbf{L}_{dq}^{a'}=\begin{bmatrix} L_s & 0 & NM_{sr} & 0 \\ 0 & L_s & 0 & NM_{sr} \\ NM_{sr} & 0 & N^2L_r & 0 \\ 0 & NM_{sr} & 0 & N^2L_r \end{bmatrix} \tag{36}$$

Then, the flux-linkage matrix becomes

$$\begin{bmatrix} \psi_{ds}^{a} \\ \psi_{qs}^{a} \\ \psi_{dr}^{a'} \\ \psi_{qr}^{a'} \end{bmatrix}=\begin{bmatrix} L_s & 0 & L_m & 0 \\ 0 & L_s & 0 & L_m \\ L_m & 0 & L_r' & 0 \\ 0 & L_m & 0 & L_r' \end{bmatrix}\begin{bmatrix} i_{ds}^{a} \\ i_{qs}^{a} \\ i_{dr}^{a'} \\ i_{qr}^{a'} \end{bmatrix} \tag{37}$$

The stator and rotor voltage equations and flux-linkage equations in the arbitrary reference frame are written by using Eqs. (33) and (37), respectively. It follows that these equations are suitable for simulating the operation of induction machines and for designing various control schemes.

3. Space-Phasor Representation of Equations

In this section, the voltage and flux-linkage space-phasor equations will be presented only in the arbitrary reference frame. Then, the space-phasor of the stator quantities (current, voltage, flux-linkage) are described through their direct- and quadrature-axis components in the arbitrary reference frame as

$$\vec{\mathbf{i}}_s=i_{ds}^{a}+ji_{qs}^{a} \quad , \quad \vec{\mathbf{u}}_s=u_{ds}^{a}+ju_{qs}^{a} \quad , \quad \vec{\boldsymbol{\psi}}_s=\psi_{ds}^{a}+j\psi_{qs}^{a} \tag{38}$$

and similarly

$$\vec{\mathbf{i}}_r'=i_{dr}^{a'}+ji_{qr}^{a'} \quad , \quad \vec{\mathbf{u}}_r'=u_{dr}^{a'}+ju_{qr}^{a'} \quad , \quad \vec{\boldsymbol{\psi}}_r'=\psi_{dr}^{a'}+j\psi_{qr}^{a'} \tag{39}$$

Using the above definitions of the current and flux-linkage space-phasors, the stator and rotor flux-linkage equations in Eq. (37) can be put into the following space-phasor form:

$$\vec{\boldsymbol{\psi}}_s=L_s\vec{\mathbf{i}}_s+L_m\vec{\mathbf{i}}_r' \tag{40.a}$$

$$\vec{\boldsymbol{\psi}}_r'=L_r'\vec{\mathbf{i}}_r'+L_m\vec{\mathbf{i}}_s \tag{40.b}$$

Similar space-phasor forms of the voltage equations can be derived from Eq. (33). Then, by utilizing the space-phasor definitions and equations in Eqs. (38), (39), and (40), the stator and rotor voltage equations can be put into the following space-phasor form:

$$\vec{\mathbf{u}}_s = R_s\vec{\mathbf{i}}_s + \frac{d\vec{\boldsymbol{\psi}}_s}{dt} + j\omega_a\vec{\boldsymbol{\psi}}_s \tag{41.a}$$

$$\vec{\mathbf{u}}_r' = R_r'\vec{\mathbf{i}}_r' + \frac{d\vec{\boldsymbol{\psi}}_r'}{dt} + j(\omega_a - p\omega_m)\vec{\boldsymbol{\psi}}_r' \tag{41.b}$$

The per-phase equivalent circuit for an induction machine is shown in Fig. 4a, where the space-phasor quantities are given. The direct- and quadrature-axis equivalent circuits are also illustrated in Fig. 4b and 4c, respectively. In these equivalent circuits, the rotor terminals are short-circuited, i.e., $\vec{\mathbf{u}}_r' = 0$. This means that the induction machine under consideration has a squirrel-cage-type rotor.

4. State-Space Equations in Arbitrary Reference Frame

The stator voltages and currents can be directly sensed from the fixed stator windings. Similarly, the rotor voltages and currents can be measured from the rotating rotor windings, but it is almost impossible in the case of a squirrel-cage-type rotor. Therefore, the rotor currents are not preferred as the state variables in the state-space machine models. However, the stator and rotor flux-linkages can be chosen as state variables since they can be observed from measurable quantities. In this case, three different state-space models of the machine can be derived according to the state variables to be selected. For this study, the state variables were taken for Models #1, #2, and #3 as follows:

Model #1: The space-phasor of the stator current $\vec{\mathbf{i}}_s$ and the space-phasor of the stator flux-linkage $\vec{\boldsymbol{\psi}}_s$ are selected as the state variables. From Eq. (41.a), we obtain

$$\frac{d\vec{\boldsymbol{\psi}}_s}{dt} = -R_s\vec{\mathbf{i}}_s - j\omega_a\vec{\boldsymbol{\psi}}_s + \vec{\mathbf{u}}_s \tag{42}$$

From Eqs. (40.a) and (40.b), we have

$$\vec{\mathbf{i}}_r' = \frac{1}{L_m}\vec{\boldsymbol{\psi}}_s - \frac{L_s}{L_m}\vec{\mathbf{i}}_s \tag{43.a}$$

$$\vec{\boldsymbol{\psi}}_r' = \frac{L_r'}{L_m}\vec{\boldsymbol{\psi}}_s - \sigma\frac{L_sL_r'}{L_m}\vec{\mathbf{i}}_s \tag{43.b}$$

where $\sigma = 1 - (L_m^2 / L_s L_r')$ is the total leakage factor. Firstly, Eqs. (43.a) and (43.b) are substituted into Eq. (41.b) and subsequently if it is rearranged with Eq. (42) for $\vec{\mathbf{u}}_r' = 0$, it yields

$$\frac{d\vec{\mathbf{i}}_s}{dt} = \left[-\left(\frac{R_s}{\sigma L_s} + \frac{1}{\sigma \tau_r}\right) - j(\omega_a - p\omega_m)\right]\vec{\mathbf{i}}_s + \left(\frac{1}{\sigma L_s \tau_r} - jp\omega_m \frac{1}{\sigma L_s}\right)\vec{\boldsymbol{\psi}}_s + \frac{1}{\sigma L_s}\vec{\mathbf{u}}_s \tag{44}$$

where $\tau_r = L_r'/R_r'$ is the rotor time-constant. The state-space equations are now represented by Eqs. (42) and (44). When these space-phasors are expanded by using the phasor definitions of $\vec{\mathbf{u}}_s$, $\vec{\mathbf{i}}_s$ and $\vec{\boldsymbol{\psi}}_s$ in Eq. (38), the machine model is written by

$$\frac{d}{dt}\begin{bmatrix} \bar{\imath}_{dqs}^a \\ \bar{\psi}_{dqs}^a \end{bmatrix} = \begin{bmatrix} \mathbf{A}_{11} & \mathbf{A}_{12} \\ \mathbf{A}_{21} & \mathbf{A}_{22} \end{bmatrix}\begin{bmatrix} \bar{\imath}_{dqs}^a \\ \bar{\psi}_{dqs}^a \end{bmatrix} + \begin{bmatrix} \mathbf{B}_1 \\ \mathbf{B}_2 \end{bmatrix}\bar{u}_{dqs}^a \quad , \quad \bar{\imath}_{dqs}^a = \mathbf{C}\begin{bmatrix} \bar{\imath}_{dqs}^a \\ \bar{\psi}_{dqs}^a \end{bmatrix} \tag{45}$$

The output **C** matrix and the sub-matrices of the system **A** and input **B** matrices are given in Table 1, where the matrices **I**, **J** and **0** that expand the terms are as in

$$\mathbf{I} = \begin{bmatrix} 1 & 0 \\ 0 & 1 \end{bmatrix} \quad , \quad \mathbf{J} = \begin{bmatrix} 0 & -1 \\ 1 & 0 \end{bmatrix} \quad , \quad \mathbf{0} = \begin{bmatrix} 0 & 0 \\ 0 & 0 \end{bmatrix}$$

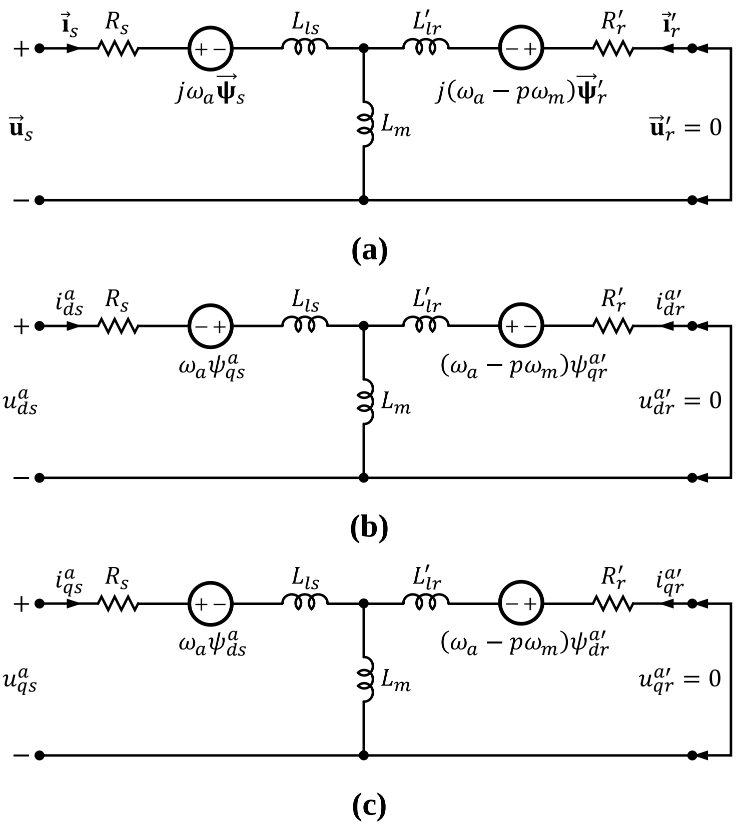

Figure 4. Per-phase equivalent circuit in the arbitrary reference frame; **(a)** space-phasor equivalent circuit, **(b)** direct-axis equivalent circuit, **(c)** quadrature-axis equivalent circuit

Model #2: The space-phasor of the stator current $\vec{\mathbf{i}}_s$ and the space-phasor of the rotor flux-linkage $\vec{\boldsymbol{\psi}}'_r$ are selected as the state variables. From Eqs. (40.a) and (40.b), we obtain

$$\vec{\mathbf{i}}'_r = \frac{1}{L'_r}\vec{\boldsymbol{\psi}}'_r - \frac{L_m}{L'_r}\vec{\mathbf{i}}_s \tag{46.a}$$

$$\vec{\boldsymbol{\psi}}_s = \frac{L_m}{L'_r}\vec{\boldsymbol{\psi}}'_r + \sigma L_s\vec{\mathbf{i}}_s \tag{46.b}$$

Firstly, if substituting Eq. (46.a) into Eq. (41.b), (for $\vec{\mathbf{u}}'_r = 0$) it results in

$$\frac{d\vec{\boldsymbol{\psi}}'_r}{dt} = \frac{L_m}{\tau_r}\vec{\mathbf{i}}_s + \left[-\frac{1}{\tau_r} - j(\omega_a - p\omega_m)\right]\vec{\boldsymbol{\psi}}'_r \tag{47}$$

Secondly, Eq. (46.b) is substituted into Eq. (41.a) and then if the obtained is rearranged with Eq. (47), we have

$$\frac{d\vec{\mathbf{i}}_s}{dt} = -\left(\frac{R_s}{\sigma L_s} + \frac{1-\sigma}{\sigma\tau_r} + j\omega_a\right)\vec{\mathbf{i}}_s + \frac{L_m}{\sigma L_s L'_r}\left(\frac{1}{\tau_r} - jp\omega_m\right)\vec{\boldsymbol{\psi}}'_r + \frac{1}{\sigma L_s}\vec{\mathbf{u}}_s \tag{48}$$

The system of differential equations is now represented by Eqs. (47) and (48). When the space-phasors are expanded by using the phasor definitions of $\vec{\mathbf{u}}_s$, $\vec{\mathbf{i}}_s$ and $\vec{\boldsymbol{\psi}}'_r$ in Eqs. (38) and (39), the machine model is written by

$$\frac{d}{dt}\begin{bmatrix}\bar{\imath}^a_{dqs}\\ \bar{\psi}^{a\prime}_{dqr}\end{bmatrix} = \begin{bmatrix}\mathbf{A}_{11} & \mathbf{A}_{12}\\ \mathbf{A}_{21} & \mathbf{A}_{22}\end{bmatrix}\begin{bmatrix}\bar{\imath}^a_{dqs}\\ \bar{\psi}^{a\prime}_{dqr}\end{bmatrix} + \begin{bmatrix}\mathbf{B}_1\\ \mathbf{B}_2\end{bmatrix}\bar{u}^a_{dqs} \quad , \quad \bar{\imath}^a_{dqs} = \mathbf{C}\begin{bmatrix}\bar{\imath}^a_{dqs}\\ \bar{\psi}^{a\prime}_{dqr}\end{bmatrix} \tag{49}$$

where the output **C** matrix and the sub-matrices of **A** and **B** are given in Table 1.

Model #3: The space-phasor of the stator flux-linkage $\vec{\boldsymbol{\psi}}_s$ and the space-phasor of the rotor flux-linkage $\vec{\boldsymbol{\psi}}'_r$ are selected as the state variables. From Eqs. (40.a) and (40.b), we obtain

$$\vec{\mathbf{i}}_s = \frac{1}{\sigma L_s}\vec{\boldsymbol{\psi}}_s + \frac{\sigma - 1}{\sigma L_m}\vec{\boldsymbol{\psi}}'_r \tag{50.a}$$

$$\vec{\mathbf{i}}'_r = \frac{\sigma - 1}{\sigma L_m}\vec{\boldsymbol{\psi}}_s + \frac{1}{\sigma L'_r}\vec{\boldsymbol{\psi}}'_r \tag{50.b}$$

Table 1. Sub-matrices of the system **A** and input **B** matrices, and the output **C** matrix for the state-space models #1, #2, and #3

Model #1

$$\mathbf{x} = \left[\bar{\imath}_{dqs}^{a} \;\; \bar{\psi}_{dqs}^{a}\right]^{t} \text{ where } \bar{\imath}_{dqs}^{a} = \left[i_{ds}^{a} \;\; i_{qs}^{a}\right]^{t} \text{ and } \bar{\psi}_{dqs}^{a} = \left[\psi_{ds}^{a} \;\; \psi_{qs}^{a}\right]^{t}$$

$$\mathbf{A} = \begin{bmatrix} -\left(\frac{R_s}{\sigma L_s} + \frac{1}{\sigma \tau_r}\right)\mathbf{I} - (\omega_a - p\omega_m)\mathbf{J} & \frac{1}{\sigma L_s \tau_r}\mathbf{I} - p\omega_m \frac{1}{\sigma L_s}\mathbf{J} \\ -R_s\mathbf{I} & -\omega_a\mathbf{J} \end{bmatrix} \quad , \quad \mathbf{B} = \begin{bmatrix} \frac{1}{\sigma L_s}\mathbf{I} \\ \mathbf{I} \end{bmatrix}$$

$$\mathbf{C} = [\mathbf{I} \quad \mathbf{0}]$$

Model #2

$$\mathbf{x} = \left[\bar{\imath}_{dqs}^{a} \;\; \bar{\psi}_{dqr}^{a\prime}\right]^{t} \text{ where } \bar{\imath}_{dqs}^{a} = \left[i_{ds}^{a} \;\; i_{qs}^{a}\right]^{t} \text{ and } \bar{\psi}_{dqr}^{a\prime} = \left[\psi_{dr}^{a\prime} \;\; \psi_{qr}^{a\prime}\right]^{t}$$

$$\mathbf{A} = \begin{bmatrix} -\left(\frac{R_s}{\sigma L_s} + \frac{1-\sigma}{\sigma \tau_r}\right)\mathbf{I} - \omega_a\mathbf{J} & \frac{L_m}{\sigma L_s L_r'}\left(\frac{1}{\tau_r}\mathbf{I} - p\omega_m\mathbf{J}\right) \\ \frac{L_m}{\tau_r}\mathbf{I} & -\frac{1}{\tau_r}\mathbf{I} - (\omega_a - p\omega_m)\mathbf{J} \end{bmatrix} \quad , \quad \mathbf{B} = \begin{bmatrix} \frac{1}{\sigma L_s}\mathbf{I} \\ \mathbf{0} \end{bmatrix}$$

$$\mathbf{C} = [\mathbf{I} \quad \mathbf{0}]$$

Model #3

$$\mathbf{x} = \left[\bar{\psi}_{dqs}^{a} \;\; \bar{\psi}_{dqr}^{a\prime}\right]^{t} \text{ where } \bar{\psi}_{dqs}^{a} = \left[\psi_{ds}^{a} \;\; \psi_{qs}^{a}\right]^{t} \text{ and } \bar{\psi}_{dqr}^{a\prime} = \left[\psi_{dr}^{a\prime} \;\; \psi_{qr}^{a\prime}\right]^{t}$$

$$\mathbf{A} = \begin{bmatrix} -\frac{R_s}{\sigma L_s}\mathbf{I} - \omega_a\mathbf{J} & R_s \frac{1-\sigma}{\sigma L_m}\mathbf{I} \\ R_r' \frac{1-\sigma}{\sigma L_m}\mathbf{I} & -\frac{1}{\sigma \tau_r}\mathbf{I} - (\omega_a - p\omega_m)\mathbf{J} \end{bmatrix} \quad , \quad \mathbf{B} = \begin{bmatrix} \mathbf{I} \\ \mathbf{0} \end{bmatrix}$$

$$\mathbf{C} = \begin{bmatrix} \frac{1}{\sigma L_s}\mathbf{I} & \frac{\sigma - 1}{\sigma L_m}\mathbf{I} \end{bmatrix}$$

In a similar manner to the previous algebraic manipulations, by using Eqs. (50.a) and (50.b), the system of differential equations is obtained from Eqs. (41.a) and (41.b) as follows:

$$\frac{d\vec{\boldsymbol{\psi}}_s}{dt} = \left(-\frac{R_s}{\sigma L_s} - j\omega_a\right)\vec{\boldsymbol{\psi}}_s + R_s \frac{1-\sigma}{\sigma L_m}\vec{\boldsymbol{\psi}}_r' + \vec{\mathbf{u}}_s \tag{51}$$

$$\frac{d\vec{\boldsymbol{\psi}}_r'}{dt} = R_r' \frac{1-\sigma}{\sigma L_m}\vec{\boldsymbol{\psi}}_s + \left[-\frac{1}{\sigma \tau_r} - j(\omega_a - p\omega_m)\right]\vec{\boldsymbol{\psi}}_r' \tag{52}$$

and the above space-phasors are expanded as

$$\frac{d}{dt}\begin{bmatrix}\bar{\psi}_{dqs}^{a}\\ \bar{\psi}_{dqr}^{a\prime}\end{bmatrix}=\begin{bmatrix}\mathbf{A}_{11} & \mathbf{A}_{12}\\ \mathbf{A}_{21} & \mathbf{A}_{22}\end{bmatrix}\begin{bmatrix}\bar{\psi}_{dqs}^{a}\\ \bar{\psi}_{dqr}^{a\prime}\end{bmatrix}+\begin{bmatrix}\mathbf{B}_{1}\\ \mathbf{B}_{2}\end{bmatrix}\bar{u}_{dqs}^{a}\quad,\quad \bar{\imath}_{dqs}^{a}=\mathbf{C}\begin{bmatrix}\bar{\psi}_{dqs}^{a}\\ \bar{\psi}_{dqr}^{a\prime}\end{bmatrix} \tag{53}$$

where the output matrix and the sub-matrices are given in Table 1.

5. Electromagnetic Torque in Induction Machine

The main output variables of the machine are the produced torque t_e and the rotor mechanical speed ω_m. The mechanical output power P_m is also equal to $\mathrm{t}_e\omega_m$ or $\mathrm{t}_e\omega_r/p$ for $p>1$. Then, the produced torque is defined as

$$\mathrm{t}_e=p\frac{\mathrm{P}_m}{\omega_r} \tag{54}$$

The mechanical output power can be derived from the instantaneous value of the input power supplied to the machine by considering the principle of conservation of energy. The definition of the output power is first obtained for the three-phase model. Thereafter, the relevant transformations are applied, and their corresponding expressions to the other two-phase models are found. After some complex algebraic operations, the output power in the arbitrary reference frame is obtained by

$$\mathrm{P}_m=k\cdot\left({\bar{\imath}_{dq}^{a}}^{t}\mathbf{G}_{dq(\omega_r)}^{a}\frac{d\theta_r}{dt}\bar{\imath}_{dq}^{a}\right) \tag{55}$$

where $\mathbf{G}_{dq(\omega_r)}^{a}=\mathbf{G}_{\alpha\beta}^{s}$. Using Eqs. (54) and (24), the electromagnetic torque is given as

$$\mathrm{t}_e=k\cdot pM_{sr}\left(i_{qs}^{a}i_{dr}^{a}-i_{ds}^{a}i_{qr}^{a}\right) \tag{56}$$

where k is a torque constant. For the power-invariant form of the phase transformation, $k=1$, but for the non-power-invariant case, $k=3/2$. On the other hand, when the rotor currents are reduced to the stator side, it becomes

$$\mathrm{t}_e=k\cdot pL_m\left(i_{qs}^{a}i_{dr}^{a\prime}-i_{ds}^{a}i_{qr}^{a\prime}\right) \tag{57}$$

The electromagnetic torque can also be expressed in the space-phasor form. By considering the space-phasor definitions of $\vec{\mathbf{i}}_s$ and $\vec{\mathbf{i}}_r'$, the torque equation can be put into the following form:

$$\mathrm{t}_e = k \cdot pL_m(\vec{\mathbf{i}}_r' \times \vec{\mathbf{i}}_s) \tag{58.a}$$

where × denotes the cross product of two vectors. Considering Eqs. (43.a), (46.a), and (50.a), other equivalent expressions for the electromagnetic torque can be defined as

$$\mathrm{t}_e = k \cdot p(\vec{\boldsymbol{\psi}}_s \times \vec{\mathbf{i}}_s) = k \cdot p(\psi_{ds}^a i_{qs}^a - \psi_{qs}^a i_{ds}^a) \tag{58.a}$$

$$\mathrm{t}_e = k \cdot p \frac{L_m}{L_r'}(\vec{\boldsymbol{\psi}}_r' \times \vec{\mathbf{i}}_s) = k \cdot p \frac{L_m}{L_r'}(\psi_{dr}^{a\prime} i_{qs}^a - \psi_{qr}^{a\prime} i_{ds}^a) \tag{58.b}$$

$$\mathrm{t}_e = k \cdot p \frac{L_m}{\sigma L_s L_r'}(\vec{\boldsymbol{\psi}}_r' \times \vec{\boldsymbol{\psi}}_s) = k \cdot p \frac{L_m}{\sigma L_s L_r'}(\psi_{dr}^{a\prime} \psi_{qs}^a - \psi_{qr}^{a\prime} \psi_{ds}^a) \tag{58.c}$$

where Eqs. (58.b), (58.c), and (58.d) are respectively proper torque equations for Models #1, #2, and #3. Finally, the state-space and torque equations of the machine hold under both transient and steady-state conditions. However, the equation of motion

$$\mathrm{t}_e = \mathrm{t}_l + \mathrm{J}_l \frac{d\omega_m}{dt} + \mathrm{f}_d \omega_m \tag{59}$$

is also required for transient conditions, where t_l is the load torque, J_l is the inertia of the rotor and f_d is the damping constant which denotes dissipation due to windage and friction. The motion equation introduces the relationship between the developed torque and rotor mechanical speed, and hence it is used to determine the rotor speed in simulation studies.

6. Reference Frames Used in Machine Model

The dynamic behavior of any induction machine can be simulated by using the general block diagram in Fig. 5. As seen in Fig. 5, the inputs of the model are the stator voltages and load torque. The outputs are the stator currents, developed torque, and rotor mechanical speed. The transformation angle θ_a is obtained by

$$\theta_a = \int \omega_a \, dt \tag{60}$$

where ω_a is an arbitrary angular speed. Since the state-space models in Table 1 are expressed in the reference frame rotating with an unspecified angular speed, the machine model cannot be simulated as such. To make the machine model more suitable for simulation, the state-space equations need to be re-expressed in one of the following reference frames. The main function of the "Reference Frame Selector" sub-block is to perform this operation.

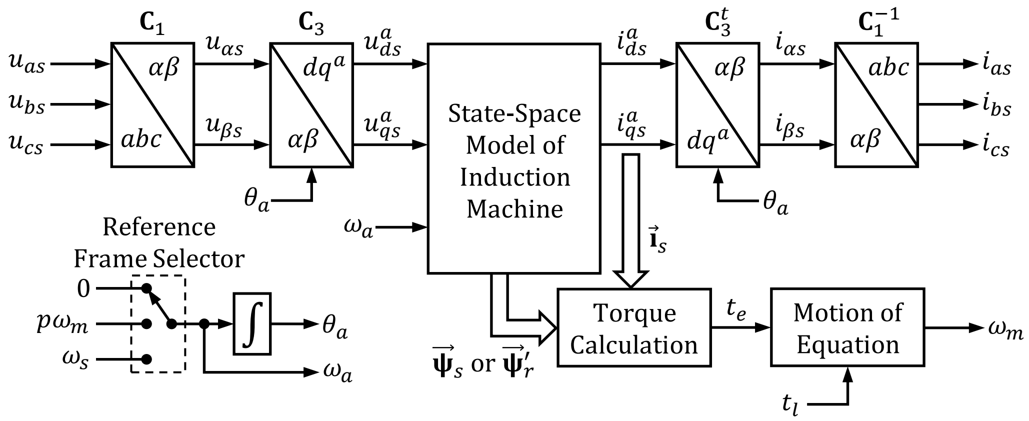

Figure 5. General simulation block diagram of an induction machine

Fig. 6 depicts commonly used reference frames in ac machine analysis. It follows that the machine model can be described in three different reference frames, namely stationary, rotor, and synchronous reference frames. How to transfer the state-space models in Table 1 from the arbitrary reference frame to other reference frames will be shown below, and their basic features will be briefly introduced.

1. The machine model is expressed in the stationary reference frame if the arbitrary reference frame coincides with the phase-a_s axis of the stator. Then, when ω_a is zero in Table 1, the state-space equations in the stationary reference frame are obtained. Since $\omega_a = 0$, the arbitrary reference frame does not rotate. Therefore, the stator and rotor quantities change sinusoidally with synchronous angular speed ω_s, where $\omega_s = 2\pi f_s$ and f_s is the fundamental frequency of the stator currents or voltages.
2. The machine model is expressed in the rotor reference frame if the arbitrary reference frame coincides with the phase-a_r axis of the rotor. Then, if ω_a is taken as ω_r or $p\omega_m$ in Table 1, the state-space equations in the rotor reference frame are achieved. Since $\omega_a = \omega_r$, the arbitrary reference frame rotates at the rotor electrical speed ω_r. Therefore, the stator and rotor quantities change sinusoidally with slip angular speed ω_{sl}, where $\omega_{sl} = \omega_s - \omega_r$.
3. The machine model is expressed in the synchronous reference frame if the arbitrary reference frame coincides with the reference frame rotating with synchronous speed ω_s. Then, if ω_a is replaced by ω_s in Table 1, the state-space equations in the synchronous reference frame are attained. Since $\omega_a = \omega_s$, the arbitrary reference frame rotates at the synchronous speed ω_s. Similarly, the stator and rotor quantities change sinusoidally with synchronous speed ω_s. Thus, these ac quantities convert into dc quantities in the synchronous reference frame.

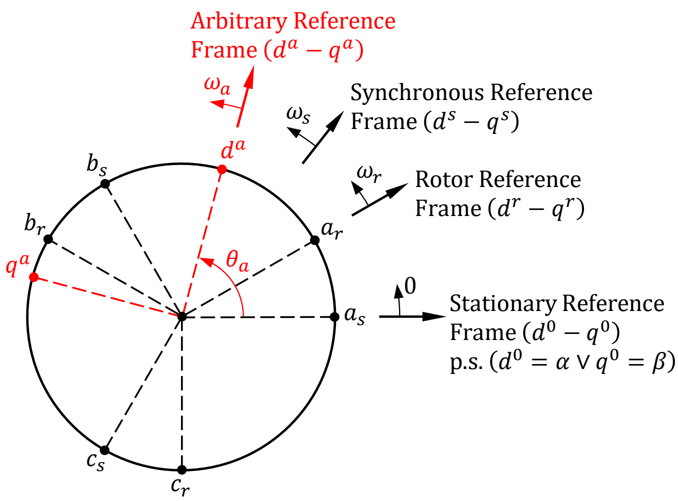

Figure 6. Commonly used reference frames in AC machine analysis

The above three reference frames provide the state-space models that can be used to analyze and/or simulate the induction machine. The most convenient reference frame is determined by the operating conditions. In general, to study balanced conditions, either the stationary or synchronously rotating reference frame is preferred rather than the rotor reference frame. However, if the stator voltages are unbalanced and the rotor voltages are balanced or zero, then the stationary reference frame is more convenient. On the contrary, if the rotor voltages are unbalanced and the stator voltages are balanced, then the rotor reference frame is more convenient. Moreover, the synchronously rotating reference frame is more useful in variable frequency applications for balanced conditions.

Table 2. Equivalent circuit and other parameters of induction machine

Parameter	Symbol	Value	Unit
Stator resistance	R_s	2.65	Ω
Rotor resistance	R_r	2.85	Ω
Stator self-inductance	L_s	0.2082	H
Rotor self-inductance	L_r	0.2122	H
Mutual inductance	L_m	0.1941	H
Number of pole-pairs	p	2	–
Moment of inertia	J_l	0.025	$\mathrm{kg \cdot m^2}$
Damping coefficient	f_d	0.001	$\mathrm{Nm \cdot s/rad}$
Rated torque	t_e	15	Nm
Rated base speed	n_m	1500	rpm

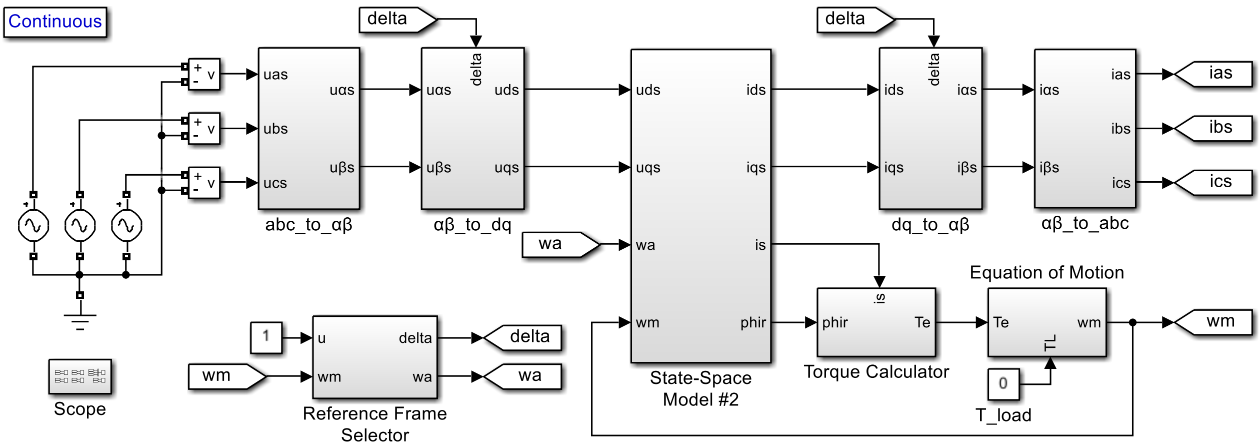

Figure 7. Simulink model of a symmetrical three-phase induction machine

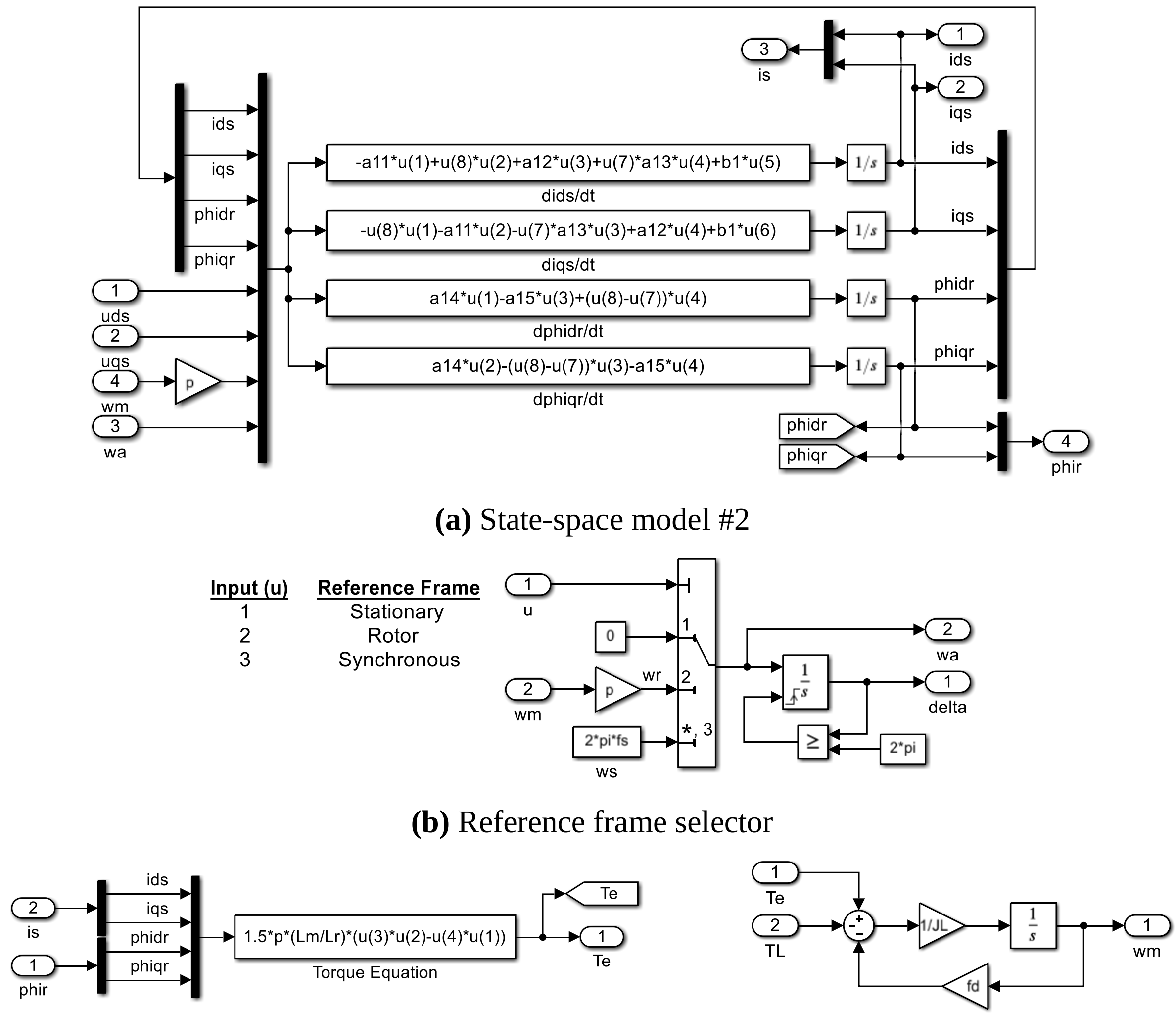

(a) State-space model #2

(b) Reference frame selector

(c) Torque calculator **(d)** Equation of motion

Figure 8. Simulink models of subsystems in the machine model

7. Simulation Studies

All the simulation studies on the presented machine models are realized in Matlab environment. The schematic simulation model and each sub-models of the machine given in Fig. 5 are created by using the blocks under Simulink library. Fig. 7 shows the simulation model of an induction machine, where its subsystem models are separately given in Fig. 8. An induction machine with 220/380V, 50Hz, 2.2kW is examined in the simulation studies. The equivalent circuit parameters are given in Table 2. The following can be said for this simulation model:

- The phase transformation is carried out by using the non-power-invariant form of $\mathbf{C}_1$; that is, while the coefficient c in Eq. (12) is taken as $2/3$ in the transformation from abc to $\alpha\beta$, $\mathbf{C}_1^{-1} = \mathbf{M}^t$ is used in the inverse transformation from $\alpha\beta$ to abc.
- The transformation angle for $\alpha\beta$ to dq and vice versa is determined under the "Reference Frame Selector" subsystem. The stationary, rotor, and synchronously rotating reference frames can be chosen when the input u is 1, 2, and 3, respectively.
- Model #2 among the state-space models in Table 1 is simulated; that is, the components of $\vec{\mathbf{i}}_s$ and $\vec{\boldsymbol{\psi}}'_r$ space-phasors are selected as the state variables. In this case, the auxiliary model parameters seen in Fig. 8a are as follows:

$$a_{11} = \frac{R_s}{\sigma L_s} + \frac{1-\sigma}{\sigma \tau_r} \quad , \quad a_{12} = \frac{L_m}{\sigma L_s L'_r}\frac{1}{\tau_r}$$

$$a_{13} = \frac{L_m}{\sigma L_s L'_r} \quad , \quad a_{14} = \frac{L_m}{\tau_r} \quad , \quad a_{15} = \frac{1}{\tau_r} \quad , \quad b_1 = \frac{1}{\sigma L_s}$$

- The developed torque is calculated by Eq. (58.c). Because this torque equation is expressed in terms of the state variables of Model #2. In addition, since the non-power-invariant form of $\mathbf{C}_1$ is applied in the phase transformation, the torque constant k is taken as $3/2$. The mechanical rotor speed is calculated by solving Eq. (59) under the "Equation of Motion" subsystem.

8. Results and Discussions

The simulations were realized for two case studies. Firstly, the free acceleration characteristic of the machine and secondly, the dynamic performance during sudden changes in the load torque are examined. For both cases, the stator windings are supplied by the rated and balanced voltages. The torque vs. speed characteristic and the machine variables during free acceleration are shown in Figs.

9a and 10a, respectively. Since the machine is initially at rest and the rated voltage is applied, the starting current and thusly the starting torque are considerably greater than their rated values. The friction and windage losses are so small that they can be neglected. Hence, the rotor shaft accelerates up to around synchronous speed and the produced torque is almost zero at this speed.

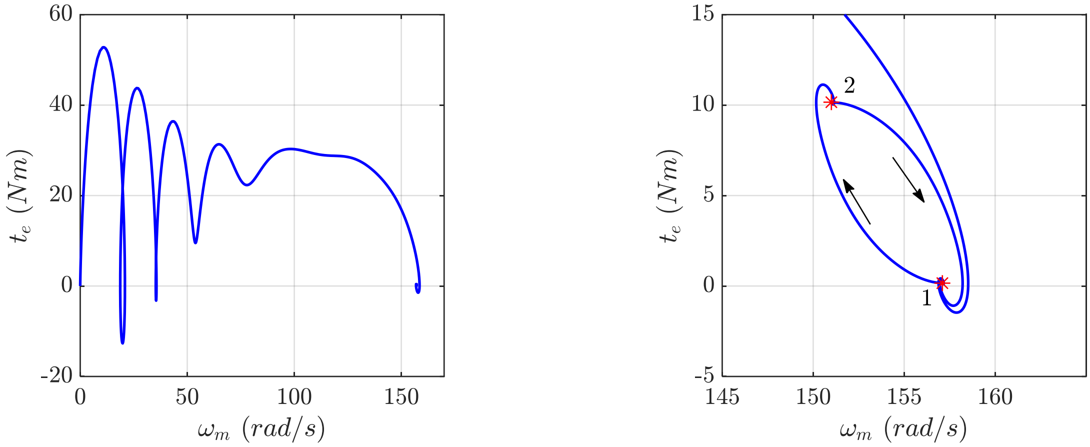

(a) **(b)**

Figure 9. Torque-speed characteristics; **(a)** during free acceleration, **(b)** during step changes in load torque from zero to 10 Nm to zero

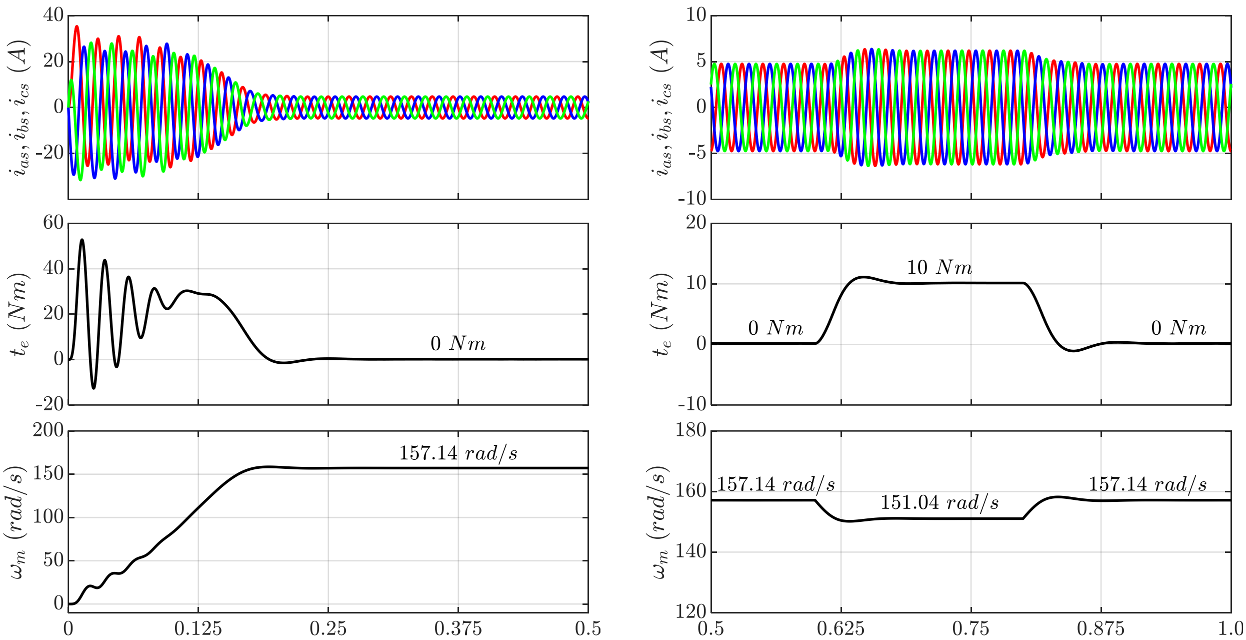

(a) **(b)**

Figure 10. Machine currents, rotor mechanical speed, and electromagnetic torque; **(a)** during free acceleration, **(b)** during step changes in load torque from zero to 10 Nm to zero

The dynamic behavior of the machine during sudden changes in the load torque is shown in Fig. 10b. Initially, (before changing the load torque), the machine is operating at synchronous speed.

The load torque is first stepped up from zero to 10 Nm and for a while, the machine is allowed to move to this new operating point. Next, the load torque is again stepped down from 10 Nm to zero. The machine returns to its original operating point. The transition trajectories between these two operating points can be seen from the torque-speed characteristic in Fig. 9b. The transition directions between the two operating points are also indicated by the arrows. Due to the characteristics of the examined machine, the machine variables approximate each operating point in an overdamped way.

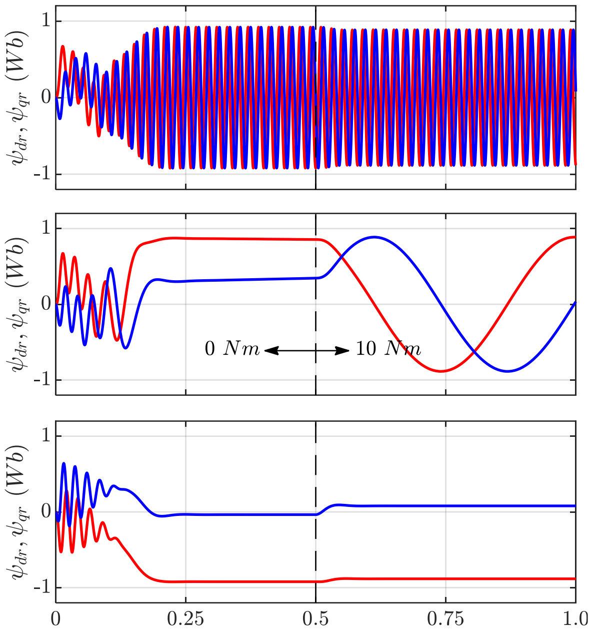

Figure 11. Variations of rotor flux-linkage components in the stationary, rotor and synchronously rotating reference frame, respectively (from top to bottom)

Finally, it will be instructive to observe the d and q components of the machine variables in various reference frames. Fig. 11 shows the components of the rotor flux-linkage in the stationary, rotor, and synchronous reference frames during two operating conditions. All the stator and rotor quantities change sinusoidally with synchronous speed in the stationary reference frame. However, these are in the form of dc quantities in the synchronous reference frame. This is respectively evident from the top and bottom figures of Fig. 11. The remaining middle figure shows the variation of the rotor flux-linkage in the rotor reference frame. These quantities change sinusoidally with slip speed. The sinusoidal changes occur in the range of a long period of time as the slip is very small initially. Under the load torque of 10 Nm, the slip increases compared to the no-load condition. Thus, the changes of these components become more pronounced depending on the increasing slip speed.

9. Conclusions

This study presents a mathematical investigation on the dynamic models of a symmetrical three-phase induction machine. All the primitive machine equations are derived in relatively simple terms by using the idea of rotating reference frame. Moreover, the ready-to-use advanced machine equations are derived in the arbitrary reference frame. The evolution of machine equations from primitive to advanced forms is presented as comprehensibly as possible and in a more compact form. This study also proposes three different state-space models derived from the advanced machine equations in the arbitrary reference frame. It is shown how to transform these state-space models from the arbitrary reference frame to the stationary, rotor, or synchronous reference frames. A general simulation block diagram is further presented which can be used in all the reference frames without any modifications to its structure. The given machine model and reference frames are discussed through some simulation studies, and the expected results are achieved. In future work, the development of vector control methods for the control of induction machines as well as observer designs for flux and speed estimation can be discussed comprehensively using the given machine models.

Statement of Research and Publication Ethics

The authors declare that all the rules required to be followed within the scope of "Higher Education Institutions Scientific Research and Publication Ethics Directive" have been complied with in all processes of the article, that The Black Sea Journal of Science and the editorial board have no responsibility for any ethical violations that may be encountered, and that this study has not been evaluated in any academic publication environment other than The Black Sea Journal of Science.

References

Abu-Rub, H., Iqbal, A., and Guzinski, J. (2012). *High performance control of ac drives with Matlab/Simulink models*. West Sussex, UK: John Wiley & Sons.

Akherraz, M. (1997). Pspice-assisted dynamic modeling and simulation of induction motor drives. *IEEE International Electric Machines and Drives Conference Record* (pp. MB1/8.1-MB1/8.3). Milwaukee, WI, USA.

Brereton, D. S., Lewis, D. G., and Young, C. G. (1957). Representation of induction-motor loads during power-system stability studies. *Transactions of the American Institute of Electrical Engineers. Part-III: Power Apparatus and Systems,* 76(3), 451-460.

Bose, B. K. (2002). *Modern power electronics and ac drives*. New Jersey, NJ: Prentice Hall.

Krause, P. C., and Thomas, C. H. (1965). Simulation of symmetrical induction machinery. *IEEE Transactions on Power Apparatus and Systems*, PAS-84(11), 1038-1053.

Krause, P. C., Wasynczuk, O., and Sudhoff, S. D. (2002). *Analysis of electric machinery and drive systems* (2nd ed.). New Jersey, NJ: IEEE Press.

Krishnan, R. (2001). *Electric motor drives – Modeling, analysis, and control*. New Jersey, NJ: Prentice Hall.

Kron, G. (1951). *Equivalent circuits of electric machinery*. New York, NY: John Wiley & Sons.

Lee, R. J., Pillay, P., and Harley, R. G. (1984). D,Q reference frames for the simulation of induction motors. *Electric Power Systems Research*, 8(1), 15-26.

Li, Q., and Hu, J. (2010). Simulation model of induction motor based on Labview. *Third International Conference on Intelligent Networks and Intelligent Systems* (pp. 273-276). Shenyang, China.

Lipo, T. A., and Consoli, A. (1984). Modeling and simulation of induction motors with saturable leakage reactances. *IEEE Transactions on Industry Applications*, IA-20(1), 180-189.

Melkebeek, J. A. (2018). *Electrical machines and drives – Fundamentals and advanced modelling*. Springer International Publishing.

Novotny, D. W., and Lipo, T. A. (1996). *Vector control and dynamics of ac drives*. New York, NY: Oxford University Press.

Ozpineci, B., and Tolbert, L. M. (2003). Simulink implementation of induction machine model – A modular approach. *IEEE International Electric Machines and Drives Conference* (pp. 728-734), Madison, WI, USA.

Park, R. H. (1929). Two-reaction theory of synchronous machines generalized method of analysis – part I. *Transactions of the American Institute of Electrical Engineers*, 48(3), 716-727.

Q'Rourke, C. J., Qasim, M. M., Overlin, M. R., and Kirtley, J. L. (2019). A geometric interpretation of reference frames and transformations: dq0, Clarke, and Park. *IEEE Transactions on Energy Conversion*, 34(4), 2070-2083.

Shi, K. L., Chan, T. F., and Wong, Y. K. (1997). Modelling of the three-phase induction motor using Simulink. *IEEE International Electric Machines and Drives Conference Record* (pp. WB3/6.1-WB3/6.3). Milwaukee, WI, USA.

Slemon, G. R. (1988). Modelling of induction machines for electric drives. *IEEE Transactions on Industry Applications*, 25(6), 1126-1131.

Stanley, H. C. (1938). An analysis of the induction machine. *Electrical Engineering*, 57(12), 751-757.

Vas, P. (1998). *Sensorless vector and direct torque control*. New York, NY: Oxford University Press.

Wack, P. (2011). *Dynamics and control of electrical drives*. Chennai, India: Springer-Verlag Berlin Heidelberg.